4.0 TASK 2. COAL LIQUEFACTION UNDER SUPERCRITICAL CONDITIONS

Over the past few years, significant interest has been expressed in a separation concept wherein a condensed phase (liquid or solid) is contacted with a fluid phase that is supercritical both in a temperature and pressure sense. Several industrial extraction processes have been developed such as deasphalting petroleum with supercritical propane (Zhuze (1960) and decaffeinating coffee with supercritical carbon dioxide, Vitzhum and Hubert (1975). Other examples would include deashing coal liquids, Baldwin et al. (1977) and regenerating activated carbon with carbon dioxide, Modell et al. (1978).

In the present study the use of supercritical fluids for coal liquefaction is investigated. In investigating these effects primary emphasis was placed on those aspects of liquefaction which would be different at supercritical conditions. The two properties of most interest are solvent density which affects the ability of the solvent to dissolve the coal and mass transfer which affects the dissolution and the degree to which solid and reactant are contacted.

Literature reviews can be found in the Ph.D. thesis and publications referred to earlier. Primary emphasis in this report will be put on solid-fluid mass transfer since the liquefaction studies were carried out as a continuation from a previous grant.

4.1 Liquefaction of Coal in Supercritical Fluids

Using a one liter stirred autoclave, Bruceton bituminous coal was liquefied in supercritical toluene at temperatures ranging from 647 to 698 K and at densities ranging from 0.157 to 0.601 g/m^3. Experiments last from 2 to 60 minutes and a coal injection technique was used. The experimental results show that the fractional

conversion of the coal to toluene soluble material increased not only with temperature but with density as well. The rate of conversion increased similarly. These results are explained by a kinetic model that postulates that toluene acts as a solvent for the reacting species although it is not a reactant itself (to a large degree). Since the degree of solubility of a solid in a supercritical fluid generally increases with temperature and density, the conversion also increases with temperature and density. By completely dissolving more of the coal, the ability of reactive species to condense into insoluble products by combining with the coal surface is decreased.

4.2 Mass Transfer at Supercritical Conditions

One of the cited advantages for using supercritical fluids as extractants is that the diffusion coefficients are significantly higher than for liquid systems while the viscosity more closely approximates that of a gas. Such trends would lead one to conclude that mass transfer characteristics of supercritical fluids may be better than for extractions carried out in the normal liquid phase.

In the pressure and temperature range where most supercritical extractions would be operated, there are no generally accepted correlations for mass tranfer coefficients. Storck and Coeuret (1980) and Wilson and Geankoplis (1966) have reviewed liquid phase relations. Both Bradshaw and Bennett (1961) and Pfeffer (1964) point out that due to the difference in Schmidt numbers, liquid and gases would be expected to have different correlations for the mass transfer coefficient.

It is the purpose of this work to measure mass transfer coefficients and to develop general correlations for determining their dependency on temperature, flow rate and pressure (or density). Although the work is done with model compounds (CO_2 naphthalene), this work provides a foundation for hypothesizing

about the effects of supercritical operating conditions on coal liquefaction characteristics.

4.2.1 Experimental Design

The schematic diagram of the experimental apparatus is shown in Figure II.1. Liquid carbon dioxide is pumped into the system via a high-pressure Milton-Roy liquid pump. Pressure is controlled by using a back pressure regulator and pressure fluctuations are dampened with an on-line surge tank.

A schematic flow diagram of the experimental apparatus is shown in Figure II.1. Liquid solvent (CO_2) is compressed by a high pressure liquid pump (Milton Roy Model A) and pumped into the system. Pressures are carefully controlled to reduce their fluctuations due to large flow rate ranges (0.88-33.45 standard liter/min at 0°C and 1.01 bar). Pressures are controlled by a back-pressure regulator (Tescom) which allows excess solvent to recycle back to the liquid pump inlet side. Fluctuations in pressure due to pumping are dampened with an on-line surge tank. Using a pressure regulator (Tescom), the system pressure is maintained within $\pm$ 0.2 bar. The pressurized solvent is preheated to the desired temperature before flowing into the bottom of the cylindrical extractor which is 3.45 cm I.D. and 14.8 cm long (upward flow). The preheater and the extractor are immersed in a water bath and the temperature is controlled to $\pm$ 0.1°C by an immersion circulator (Haake D1). Pressures and temperatures at the inlet of the extractor are measured by a pressure transmitter (Viatran 501) and a thermocouple (Type K), respectively which are connected to a data logger (Kaye Digistrip II).

The extractor is packed with a single section consisting of two layers of cylindrical naphthalene pellets which are placed between long sections of inert packing (glass beads) at the top and the bottom of the bed. The glass beads have a

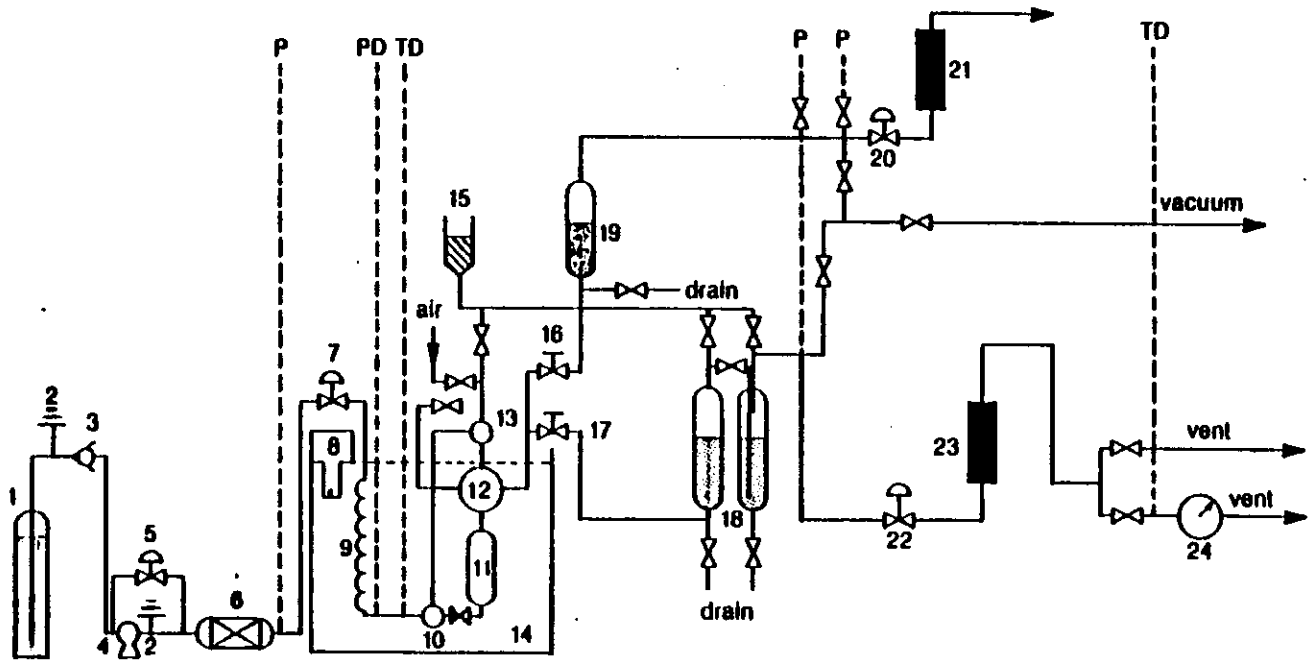

1. Liquid Co_2 cylinder
2. Relief valve
3. Check valve
4. Liquid pump
5. Back pressure regulator
6. Surge Tank
7. Pressure regulator
8. Temperature controller
9. Preheater
10. Three-way valve
11. Extractor
12. Four-way valve
13. Three-way valve
14. Water bath
15. Solvent tank
16. Metering valve
17. Metering valve
18. Sample tanks
19. Solid trap
20. Back pressure regulator
21. Rotameter
22. Back pressure regulator
23. Rotameter
24. Wet test meter

P: Pressure gauge
PD: Pressure transmitter to Data logger
TD: Thermocouple to Data logger

FIGURE II.1 Schematic Diagram of the Experimental Apparatus

diameter similar to that of the pellets. An advantage in using the inert pellets is to reduce end effects in the packed bed being used as an extractor. After extraction, the fluid mixture is expanded to atmospheric pressure through a heated metering valve (Whitey SS-31RS4) and a back-pressure regulator (Tescom). The flow rate of the fluid mixture is regulated by the metering valve. The instantaneous and total flow rates of solute-free gas are measured with a rotameter and a calibrated wet-test meter (Precision Scientific Co. Model 63125), respectively. The sample tanks are high pressure bombs which contain toluene with glass beads, which dissolve the extract (naphthalene) from the CO_2. These vessels are operated at 30 to 35 bar where the solubility of the solid in the CO_2 is near a minimum. The second vessel is redundant and is used to guarantee that all of the extract is collected and to reduce entrainment losses. No naphthalene was found in this second vessel during any experiments. Finally, the by-pass, from valve 12 to 16, is designed to insure steady-state flow through the extraction vessel 11 before samples are taken. The whole apparatus is rated for a pressure of 335 bar. All measured temperatures and pressures are recorded on a data logger at regular time intervals.

For each experimental run, the extractor is placed in the water bath with new cylinderical naphthalene pellets and the water bath is brought to the desired temperature by the temperature controller. Carbon dioxide is pressurized to the desired pressure by the liquid pump. Then carbon dioxide is slowly allowed into the extractor (11) by opening a metering valve between three-way valve (10) and extractor. Before sampling, the naphthalene-CO_2 mixture is purged through a vent (valve 16). This vent line is open for the time needed to insure that the carbon dioxide leaving the extractor has passed through the active bed (naphthalene pellets). This time can be calculated for any given experimental conditions

(temperature, pressure and flow rate of carbon dioxide). Then, with the vent line closed, the fluid mixture is allowed into the sampling section (17 to 24). The sampling time varies from 3 minutes to 1.5 hours because a large range of mass transfer rates exists between 10 atm and 200 atm. At supercritical conditions, the system is operated for about 3 minutes. After each run, all lines following the extractor are carefully cleaned with toluene to eliminate the remaining naphthalene and dried completely by air. The SCF-solid mass transfer coefficients are measured as a function of flow rate and pressure (or density). The ranges of system parameters examined in this study are shown in Table II.1. The experimental ranges of temperatures and pressures are in the region where a pure solid naphthalene can coexist with gas phase CO_2 only (Figure II.2).

Table II-1. Ranges of Experimental Parameters for the Naphthalene-CO_2 System

T= 35 - 45°C	Re = 4 - 135
P = 10.1 - 202.7, bar	Sc = 2 - 11
d_p = 0.46 - 0.61 cm	Gr = 144-4.73 x 10^7
L_T = 0.92 - 1.22, cm (2 layers)	ScGr = 313-2.0 x 10^8
ϵ = 0.406	J_d = 0.27 - 3.13
S = 9.36, cm^2	
q = 0.88 - 33.45, STD liter/min at 0°C and 1.01 bar	
μ = 1.55 x 10^4 - 8.21 x 10^{-4}, g/cm sec	
D_V = 8.38 x 10^{-5} - 3.90 x 10^{-3}, cm^2/sec	

Hard glossy naphthalene pellets are made by pouring molten naphthalene into a dye. Because the surface area of the pellets decreases during an extraction, the average area and particle diameter is used assuming that uniform extraction of the particles takes place. For a section two layers thick, this should be valid. Only a

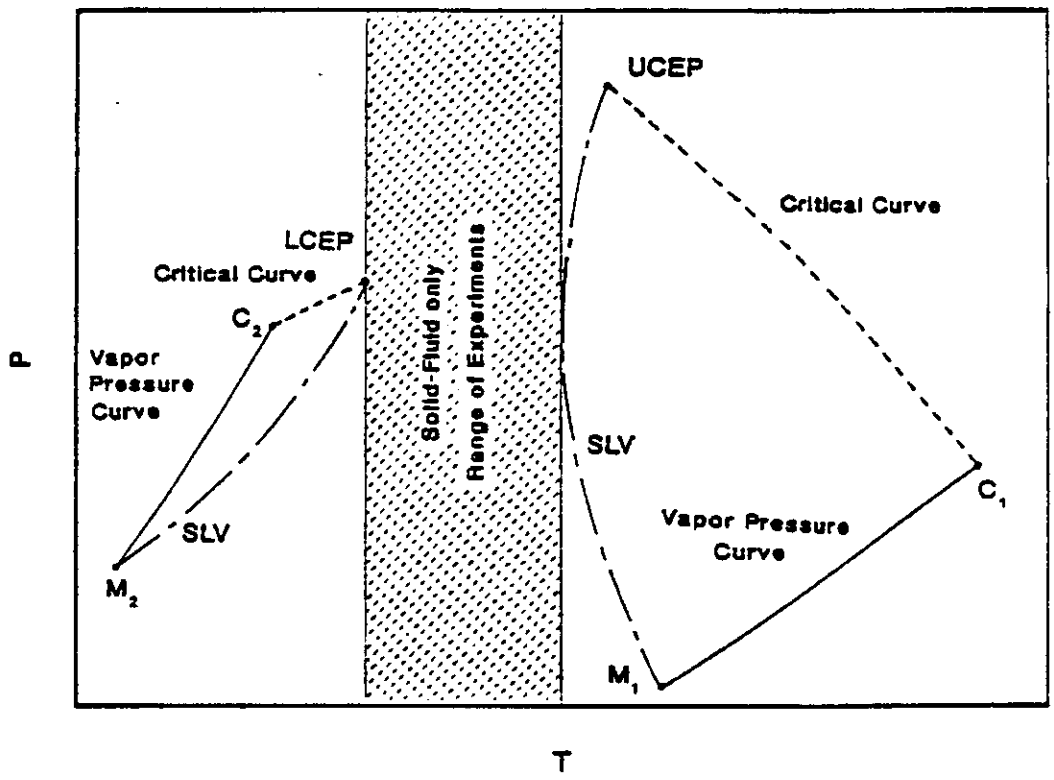

FIGURE II.2 Pressure - Temperature Phase Diagram for the Naphthalene - Carbon Dioxide System

small portion (5 to 20%) of the naphthalene was extracted, and the pellets maintained their integrity and did not break up.

Mole fractions of solid in the supercritical fluid are calculated from the weight of the collected solute and total amount of gas flow through the wet-test meter. To determine the amount of extract collected, the amount of toluene (with dissolved extract) is weighed. A sample of the toluene-extract solution is then injected into a gas chromatograph (Hewlett-Packard 5880A) to determine what portion of the solution is extract.

4.2.2 Results

Experimental results are given in Figures II.3, II.4, and II.5. In the present study, the number of cells is approximated as three for two layers of particles using the method of Krameres and Alberda and estimating the axial Peclet number to be 2 (Lim et al., 1989). The sensitivity to this cell number is checked by comparing the values of mass transfer coefficients obtained using three cells with those obtained by using a different number of cells. Representatively, for the case of n = 10, the resulting mass transfer coefficients deviate 10% (AARD) with respect to those for n = 3. For the extreme case (ideal plug flow: $n = \infty$), the deviation is only 14.2% AARD, which is the maximum possible effect of the cell number on mass transfer in packed bed. Therefore, it seems to be reasonable to use three as the number of perfect mixers for two layers of particles in the present study.

Figure II.3 shows that the mass transfer coefficients go through a maximum with respect to pressure and that at pressures below 60 bar, mass transfer coefficients are more dependent upon Re than at higher pressures. The more apparent effect of pressure on mass transfer coefficients is shown in Figure II.3 by using the correlations between mass transfer coefficient, k_y, and Reynolds number

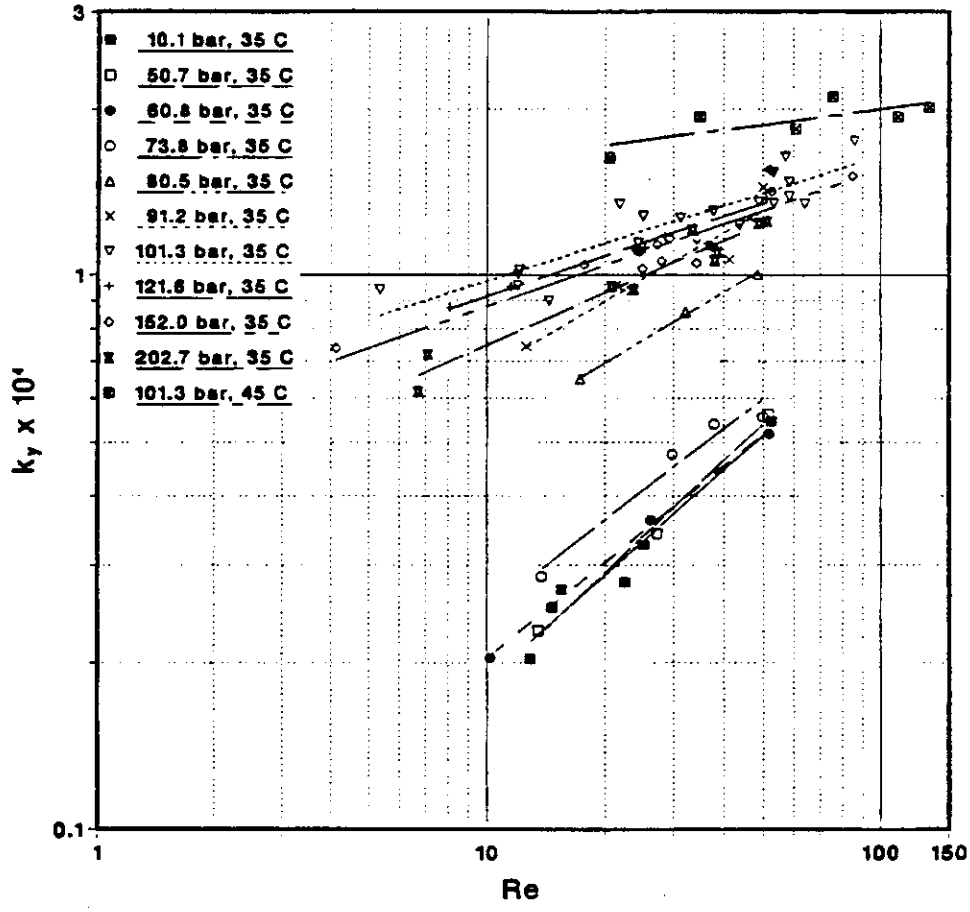

FIGURE II.3 Effect of the Reynolds Number on Mass Transfer Coefficients at Different Temperatures and Pressures

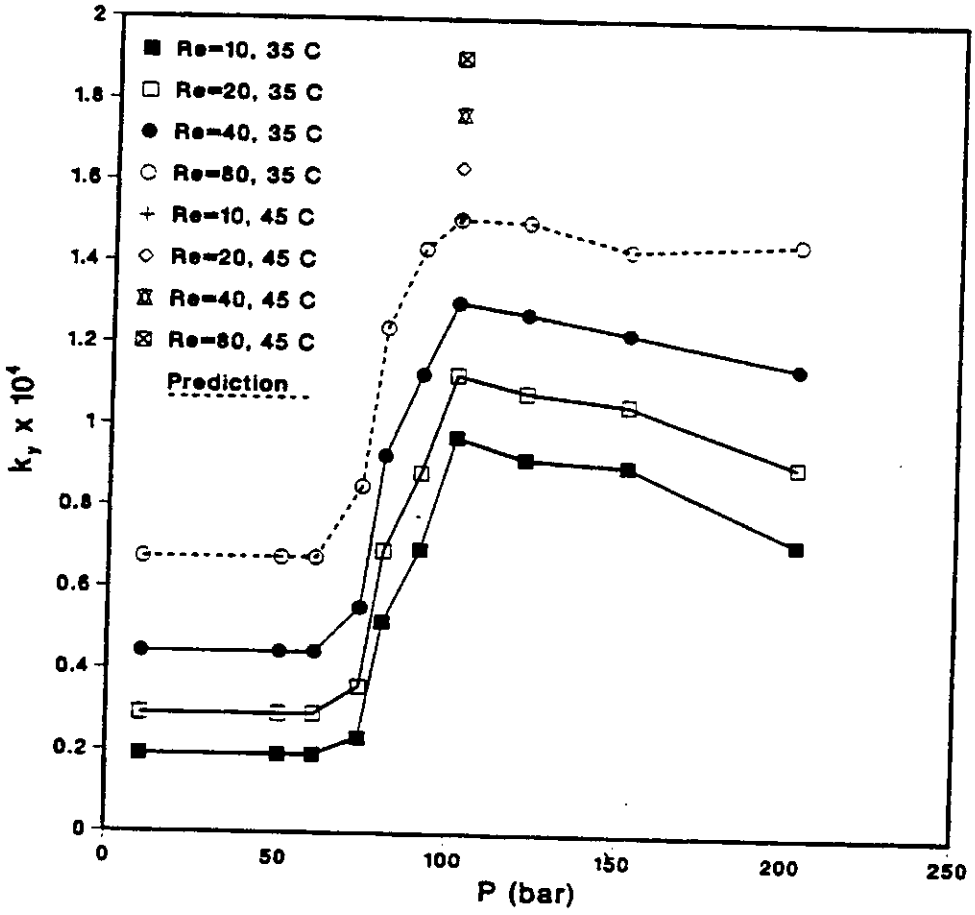

FIGURE II.4 Effect of Pressures and Temperatures on Mass Transfer Coefficients at the Same Reynolds Number

obtained from Figure II.3. Figure II.4 shows that at constant Re, the mass transfer coefficient is almost constant at low pressures below 60.8 bar. However, it increases dramatically near the critical point, has its maximum value, then it decreases gradually as the pressure increases beyond 101.3 bar. As the Reynolds number increases, forced convection becomes more important. The estimate of mass transfer coefficients at Re = 80 and 35°C shows that though there is still mass transfer enhancement at supercritical conditions (compared to at subcritical conditions) this enhancement is smaller than at lower Re. At very high Reynolds numbers, natural convection effects should be negligible and forced convection should be the dominant mass transfer mechanism. Clearly, mass transfer coefficients are much higher at supercritical conditions than at low pressure (1.01 bar and 25°C: Figure II.5).

Data at 45°C and 101.3 bar shows only slight dependence on Re which means natural convection is dominating the mass transfer. This observation agrees with the study at 45°C by Knaff and Schlünder (1987). These effects of natural convection on mass transfer can be attributed to the density differences between equilibrium CO_2-naphthalene mixtures and pure CO_2 at different temperatures and pressures (Figure II.6).

4.2.3 Mass Transfer Correlations

Under supercritical conditions correlations for mass transfer coefficients should be different from those for mass-transfer coefficients of solid-gas or solid-liquid systems, especially since the latter are usually measured at ambient temperature and pressure (Bradshaw and Bennett, 1961; Pfeffer, 1964).

At the interface between a soluble solid and a fluid, a saturated solution is formed and the concentration gradient between the interface and bulk fluid is the

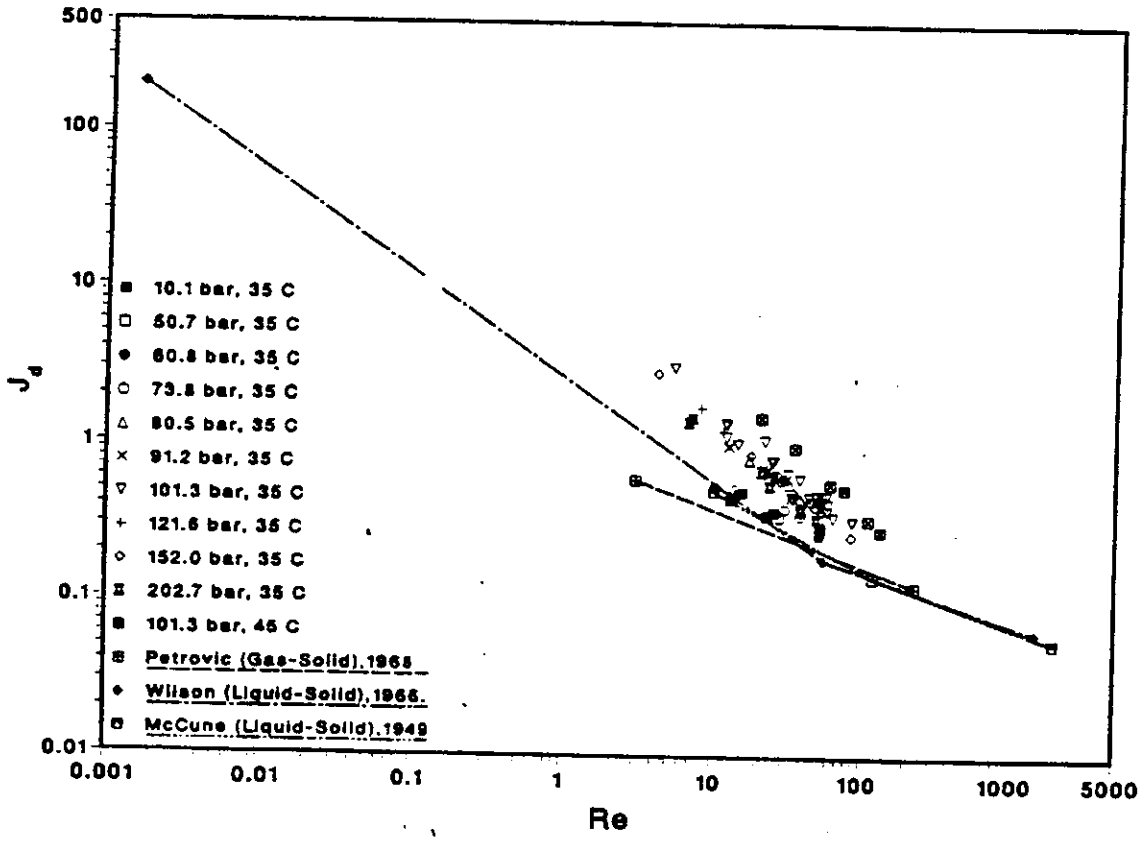

FIGURE II.5 Comparison of Mass Transfer Factor, J_d, as a Function of the Reynolds Number for Standard Conditions (25 °C and 1.01 bar)[100,101,135] and Supercritical Conditions

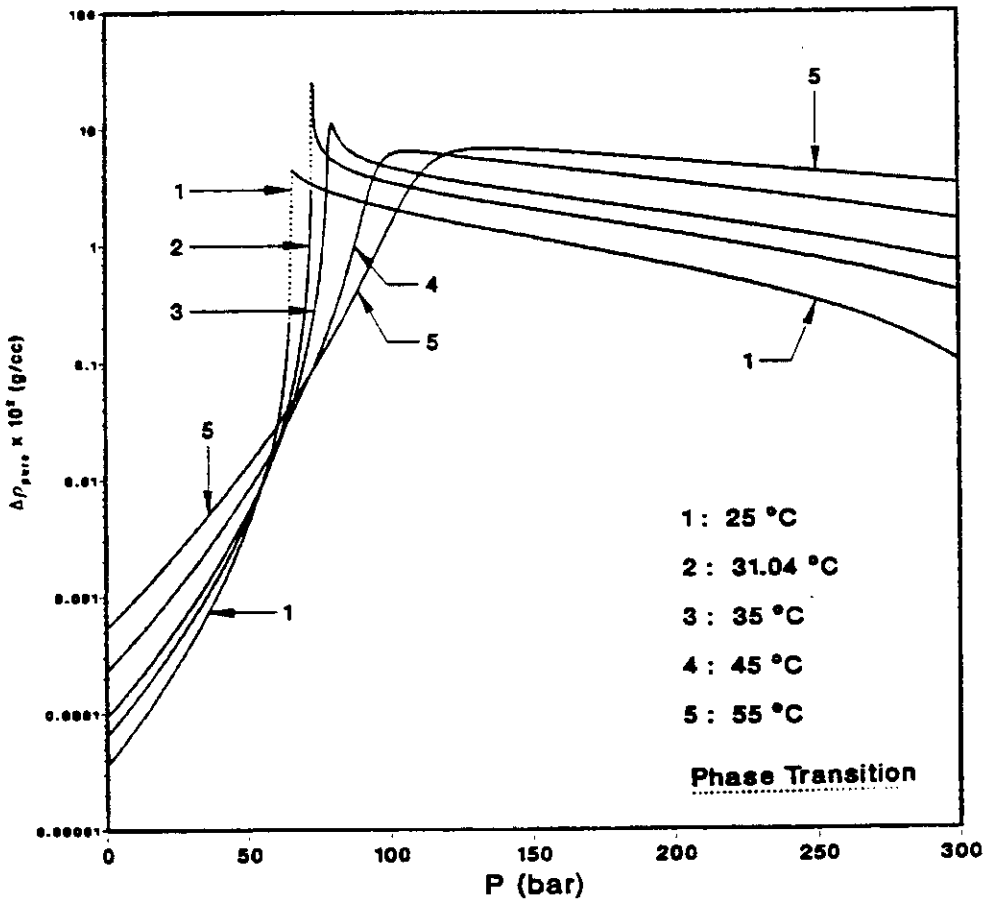

FIGURE II.6 Density Differences between Equilibrium Mixtures of Naphthalene in Carbon Dioxide and Pure Carbon Dioxide as a Function of Pressure and Temperature

driving force for mass transfer. Mass transfer of the solute into the bulk fluid occurs in three ways, depending upon the conditions. For an infinitely small solid particle in a stagnant fluid, mass transfer occurs by molecular diffusion alone, but as the size of the solid particle becomes large, natural convection currents are set up due to the density difference between the mixture at the interface and the bulk fluid. The third form of mass transfer is forced convection. All three modes of mass transfer are present in the current study.

In general, mass-transfer between a fluid and a packed bed of solid can be described by correlations of the following form:

$$Sh = f\ (Re,\ Sc,\ Gr) \qquad \text{(II-1)}$$

where Sh, Re, Sc and Gr are respectively the Sherwood number, the Reynolds number, the Schmidt number, and the Grashof number for the mass-transfer (Eckert, 1950).

Forced Convection. Under forced convection conditions, where the Grashof number is unimportant, the general expression becomes

$$Sh = f\ (Re,\ Sc) \qquad \text{(II-2)}$$

The most convenient method of correlating mass-transfer data under forced convection conditions is to plot the J_d factor (Figure II.5) as a function of Reynolds number as suggested by Colburn (1933) and Chilton and Colburn (1934) who from theoretical consideration of flow and from dimensional analysis defined J_d as follows:

$$J_d = \frac{Sh}{Re\ Sc^{1/3}} \qquad \text{(II-3)}$$

The functional dependence of J_d on Reynolds number Re has been the subject of study by many investigators. A variety of equations have been proposed to represent their experimental data. Jolls and Hanratty (1969) showed that up to Re ≈ 1000, flow over much of the surface of the packing cold be described by a boundary layer flow. According to the laminar boundary layer theory, the following correlation seems to be reasonably accurate for Sc greater than 10 Schlichting, 1968):

$$Sh = m_1\ Re^{1/2}\ Sc^{1/3} \qquad \text{(II-4)}$$

where m_1 depends upon the geometry of the packing and flow configuration. However, experiments with isolated cylinders and spheres showed that the exponent on Re in Equation (II-4) could be varied from 1/2 to 2/3, since the boundary layer hypothesis did not hold over the entire surface (Richardson, 1963). On the other hand, the exponent on Sc is usually taken as 1/3. In addition, heat transfer studies (Baldwin, 1966) at high Re suggested that for $Re \to \infty$, the exponent on Re in Equation (II-4) should be 0.7 with the same exponent on Sc, 1/3. An excellent summary and analysis of correlations for forced convection in packed beds was presented by Dwivedi and Upadhyay (1977).

Natural Convection. Recently, Debenedetti and Reid (1986) pointed out that buoyant effects had to be considered in supercritical systems because supercritical fluids have very small kinematic viscosities as a result of their high densities and low viscosities. The effect of buoyant forces can be more than two orders of magnitude higher in supercritical fluids than in normal liquids.

For transfer under natural convection conditions, where the Reynolds number is unimportant, the general expression reduces to

$$Sh = f\ (Sc,\ Gr) \tag{II-5}$$

It is reasonable to use relations which have been developed for natural convection around isolated bodies. Most work, both theoretical and practical, produces the following form:

$$Sh = m_2\ (Sc\ Gr)^{1/4} \qquad \text{for laminar natural convection} \tag{II-6}$$

$$Sh = m_3\ (Sc\ Gr)^{1/3} \qquad \text{for turbulent natural convection} \tag{II-7}$$

Merk and Prins (1954) suggested $m_2 = 0.558$ for heat transfer from a sphere. In the case of large Schmidt numbers (usually for liquid systems), Karabelas et al. (1971) proposed that $m_2 = 0.46$ and $m_3 = 0.112$ for natural convection using asymptotic relations.

If natural convection is dominant, the correlations such as those above, are likely to be appropriate for modeling the mass-transfer coefficient data. Its main characteristic is that it is independent of Reynolds number.

Combined Forced and Natural Convection. In the intermediate region where natural and forced convection happen simultaneously, neither the Reynolds number nor the Grashof number can be neglected. In the present work, it is clear that both effects are important.

Most studies reported were substantially based on the following form for assisting flows:

$$Sh_T^n = Sh_F^n + Sh_N^n \qquad \text{for assisting flows} \tag{II-8}$$

where the subscripts T, F and N indicate average total, forced and natural convection, respectively. Churchill (1977) chose 3 as an optimal value of n for assisting flows through an empirical correlation procedure. The theoretical basis for this value of 3 was given by Ruckenstein and Rajagopalan (1980) and Jorne (1984).

In this study, forced and natural convection effects oppose each other and the theoretical and experimental analysis is more complicated. Ruckenstein and Rajagopalan (1980) extended their results for the case of assisting flows to the case of opposing flows by simply replacing the plus sign in Equation II-(8) with the minus sign:

$$Sh_T^n = Sh_F^n - Sh_N^n \qquad \text{for opposing flows} \tag{II-9}$$

Jorne and Cheng (1987) also derived theoretical solutions for mass transfer coefficients by using superimposition of velocity and Lighthill transformations for both assisting and opposing flows along vertical walls.

4.2.4 Correlations

Neither Equations (II-4) or (II-6) can successfully correlate all the present experimental data even though for each pressure either of the two correlations above can be applied with moderate relative success. For example, at low pressures (35°C and 10.1-60.8 bar) where laminar forced convection is dominant, the mass transfer correlation can be expressed by an equation of the same form as Equation (II-4) with m_1 = 1.874 (7.0% AARD). At 45°C and 101.3 bar where laminar natural convection is dominant, a correlation which has the same form as Equation (II-6) with m_2 = 0.614 is effective (3.23% AARD). Figure II.5 shows that no single line can represent all the present experimental data by a plot of J_d, mass transfer factor, vs. Reynolds number which is commonly used for pure forced convection, due to natural convection effects at supercritical conditions. Buoyant effects become important under supercritical conditions due to the small kinematic viscosities which are a consequence of the high densities and low viscosities. Consequently, it is necessary to consider both forced and natural convection when attempting to correlate mass transfer coefficients under supercritical conditions.

The correlation in Equation (II-9) was tested for combined forced and natural convection around immersed bodies by Churchill (1983) who found it to be only qualitatively correct. The experimental data for heat transfer showed that a finite total Nusselt number (total Sherwood number for mass transfer) existed even though the Nusselt numbers for natural convection and forced convection were equal, and should have canceled. Jorne (1984) derived an approximate correlation for a heated vertical wall with opposing flow. This correlation was the same as Equation (II-9) except that constant coefficients for both Sh_N and Sh_F were added. However, this correlation still predicted zero total Sherwood number for certain values of Sh_N and Sh_F.

The following correlation is proposed for opposing flows in the present study. it eliminates the possibility of a zero Sherwood number:

$$Sh_T = A \times Sh_F^B + C \mid Sh_F^n - D \times Sh_N^n \mid^{1/n} \qquad \text{(II-10)}$$

where A, B, C and D are positive constants. The first term cannot be a constant but must be a function of Sh_N or Sh_F because different sets of the two Sherwood numbers which produce the same value for the second term on the RHS in Equation (II-10) would not necessarily produce the same value of Sh_T. This is due to the fact that higher values of Sh_N and Sh_F produce greater concentration and velocity gradients across the boundary-layer, and greater instability in the flow pattern. The second term on the right hand side of Equation (II-10) represents <u>absolute</u> differences between two Sherwood numbers. The validity of this proposed correlation under extreme conditions of $Re \to 0$ and $Re \to \infty$ can be determined as described below. For the case of $Re \to 0$ ($Sh_F << Sh_N$), this correlation reduces to:

$$Sh_T = (C \times D^{1/n})\ Sh_N \qquad \text{for } (Sh_F << Sh_N)$$

The total Sherwood number (Sh_T) can have the same form as the standard natural convection Sherwood number (Sh_N) if $C \times D^{1/n} = 1.0$. On the other hand, when $Re \to \infty$ ($Sh_F >> Sh_N$), Equation (II-10) reduces to:

$$Sh_T = A\ Sh_F^B + C\ Sh_F \qquad \text{for } Re \to \infty\ (Sh_F >> Sh_N) \qquad \text{(II-11)}$$

If B = 1.0 and A + C = 1.0 Sh_T can be expressed by the standard forced convections Sherwood number (Sh_F). If B ≠ 1.0, the reduced correlation shows that the dependency of Sh_T on Re changes with increasing Re because Sh_T is only a function of Re. Therefore, the proposed correlation (Equation (II-10)) is consistent at limiting conditions (Re → 0 and Re → ∞). Using Churchill's suggesting n is assigned the value of 3.

Rearrangement and regression gives the following correlation which correlates the experimental mass transfer coefficients over the entire pressure and temperature range with 14.9% AARD, and is shown in Figure II.7.

$$\frac{Sh_T}{(ScGr)^{1/4}} = 0.1828 \left(\frac{Re^2 Sc)^{1/3}}{Gr}\right)^{1/4} (Re^{1/2}\, Sc^{1/3})^{3/4}$$

$$+ 1.1398 \left| \left(\frac{Re^2 Sc^{1/3}}{Gr}\right)^{3/4} - 0.01634 \right|^{1/3} \qquad \text{(II-12)}$$

The correlating numbers are calculated by using densities, diffusivities, and viscosities as described in the Appendix.

Note that the data at 35°C and 73.8-80.5 bar show very large deviations from the proposed correlation. These errors are due almost entirely to the fact that the experimental diffusivities drop precipitously near the LCEP. Debenedetti and Reid (1986) showed that the apparent diffusivity at supercritical conditions could be as much as 6.5 times higher than the true diffusivity (by a 90° rotation of a flat plate). Thus, the apparent diffusivity in a packed bed could be much higher than the true diffusivity, especially near the LCEP where very large clusters formed at the interface might move downward by natural convection. The shaded area in Figure II.8 shows the range over which the apparent diffusivities might change.

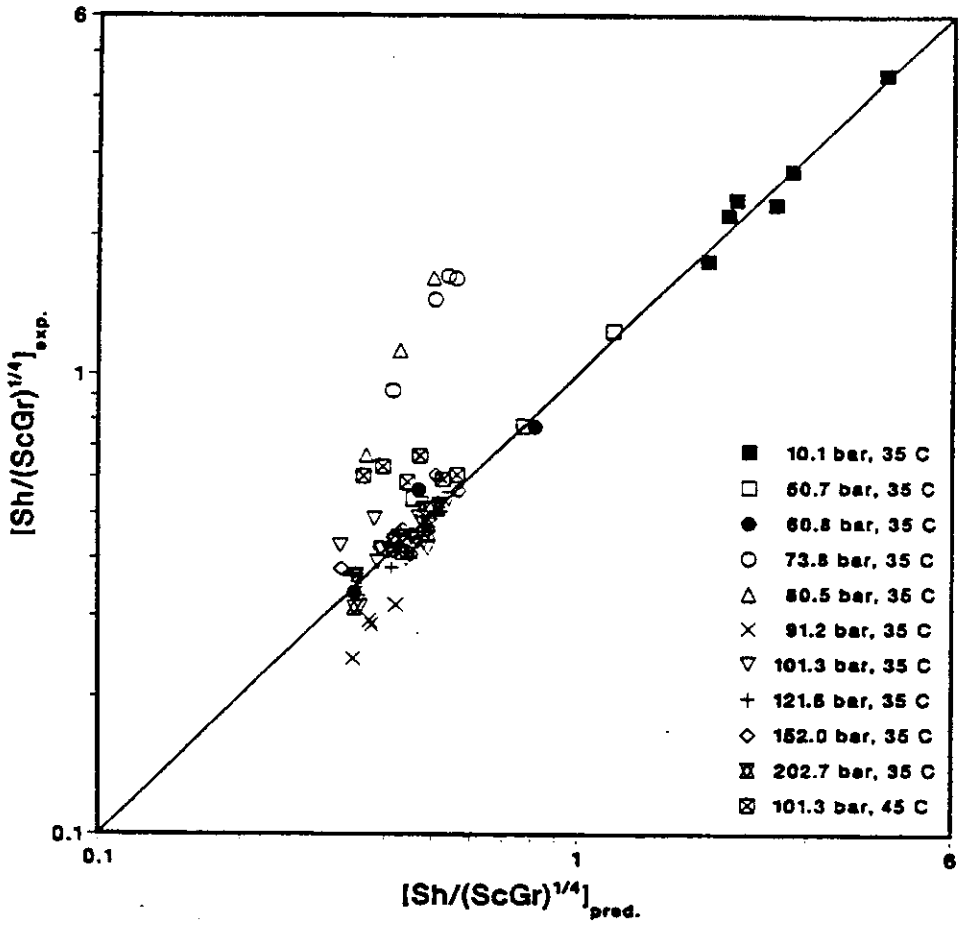

FIGURE II.7 Correlation for Combined Natural and Forced Convection in the Case of Opposing Flows

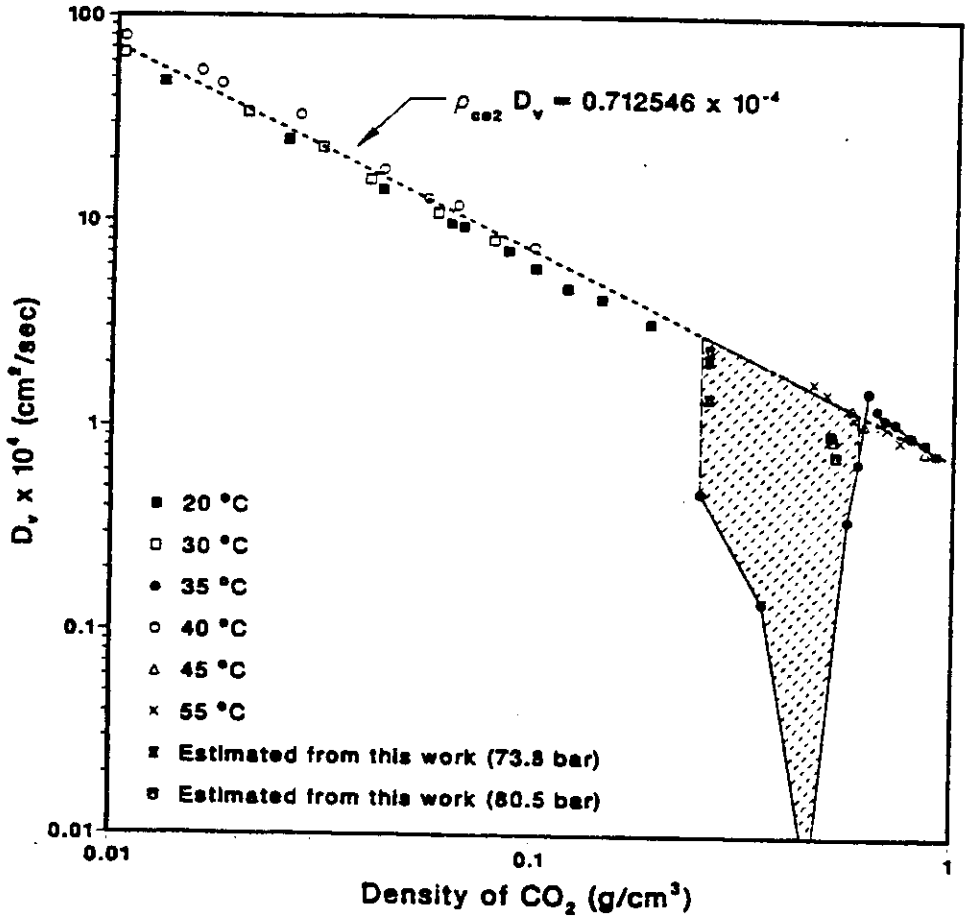

FIGURE II.8 Binary Diffusivities in the Naphthalene - Carbon Dioxide System under Subcritical to Supercritical Conditions: The shaded region is where the apparent diffusivity may be different from the true diffusivity

Accordingly, we estimated the apparent diffusitivites corresponding to each experiment at the two conditions by calculating the diffusivities which allow the experimental data to satisfy the proposed mass transfer correlation above. From Figure II.8 we can see that the estimated apparent diffusivities near the LCEP are close to the diffusivities that would be obtained by interpolating between high and low pressure diffusivity data. The following mass transfer correlation is obtained by using one overall correlation for diffusivity (Appendix) with 12.2% AARD and is shown in Figure II.9.

$$\frac{Sh_T}{(ScGr)^{1/4}} = 0.1813 \left(\frac{Re^2 Sc^{1/3}}{Gr}\right)^{1/4} (Re^{1/2} Sc^{1/3})^{3/4}$$

$$+ 1.2149 \left| \left(\frac{Re^2 Sc^{1/3}}{GR}\right)^{3/4} - 0.01649 \right|^{1/3} \qquad \text{(II-13)}$$

The experimental results obtained from the present study are compared with the supercritical mass transfer data obtained by Knaff and Schlünder (1987) for the proposed correlation Equation (II-13) in Figure II.10. It shows that considerable deviation occurs between the proposed correlation and the experimental data. The primary reasons for this is that their data were obtained at turbulent flow conditions (520 < Re < 320) in an annular duct while our data and the proposed correlation are obtained at laminar flow regime (4 < Re < 135) in a packed bed.

At Re → 0, the above correlation can be reduced to:

$$Sh_T = 0.3092 \ (Sc \ Gr)^{1/4} \qquad \text{(II-14)}$$

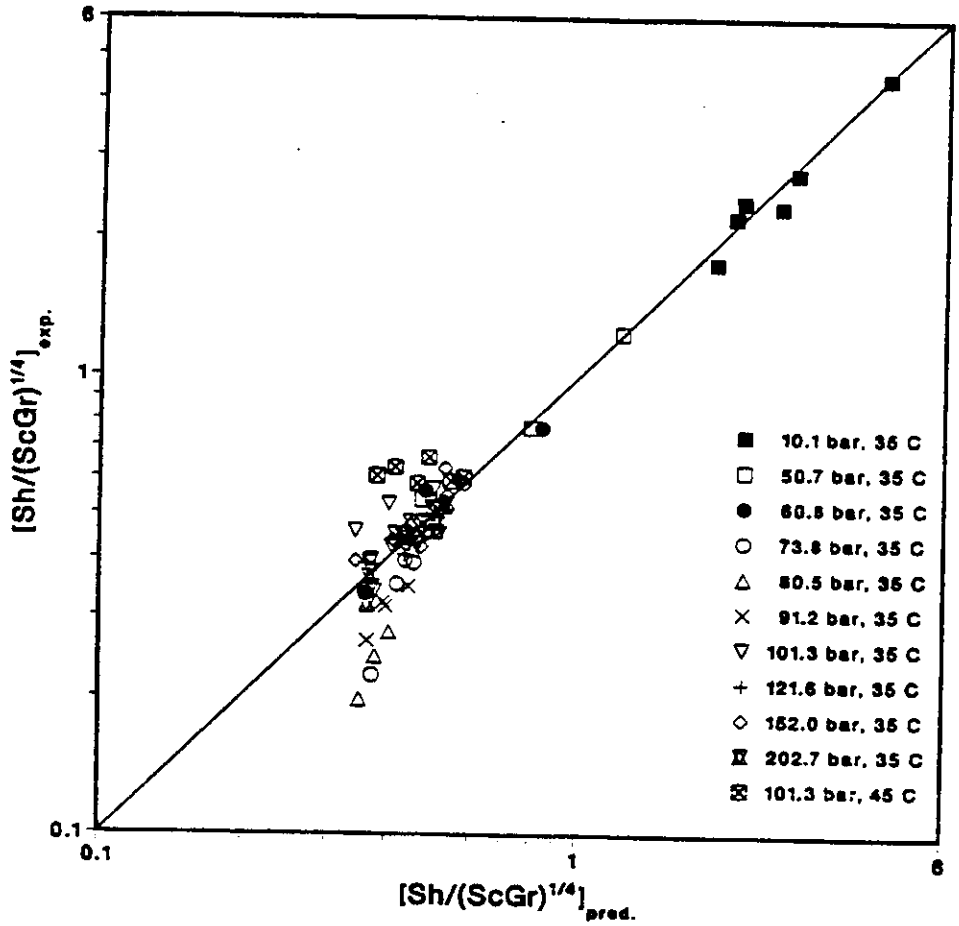

FIGURE II.9 Correlation for Combined Natural and Forced Convection in the Case of Opposing Flows (Equation 9-7): Diffusivities Obtained from Equation 7-1 for the Entire Experimental Conditions

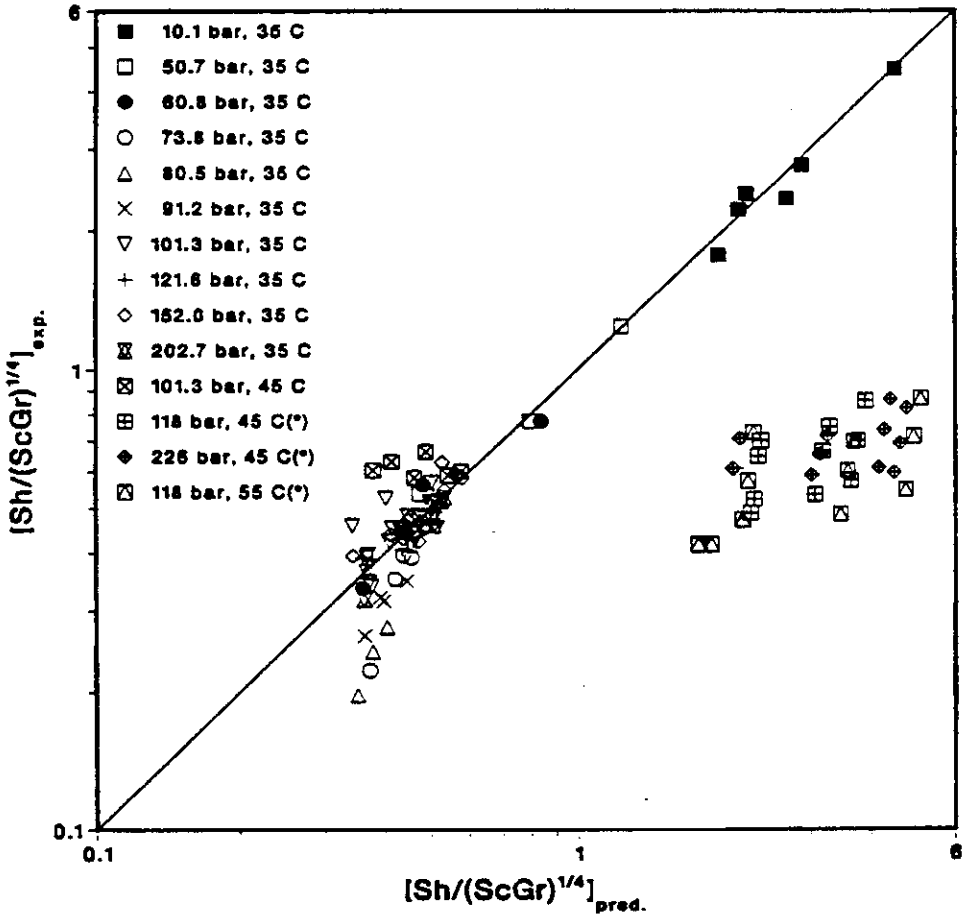

FIGURE II.10 Comparison between the Experimental Data Obtained from the Present Study and the Literature Data (*)[12] Obtained at Supercritical Conditions by Using the Proposed Correlation (Equation 9-7)

and as $Re \to \infty$, it reduces to

$$Sh_T = 0.1813\ (Re^{1/2}\ Sc^{1/3})^{7/4} + 1.2149\ Re^{1/2}\ Sc^{1/3} \qquad \text{(II-15)}$$

Additional data could be useful in assessing the range of validity for the proposed relationship. Even though the experimental data near the critical point can be correlated by using the estimated apparent diffusitivies, the correlation has uncertainties in this region due to the high sensitivity of the physical properties, especially diffusivities and equilibrium solubilities, to pressure and temperature.

In the present study, we assume that temperature at interface between the solid and the bulk fluid is equal to that in the bulk fluid. However, Knaff and Schlunder indicated that the temperature at the interface may be as much as 1°C higher or lower than the bulk depending upon whether the dissolution process was exothermic or endothermic. The calculation of the heat of dissolution shows that the dissolution is endothermic except at 73.8-90.2 bar (35°C) and 101.3 bar (45°C) for the present experimental conditions. The estimated effect of the temperature change at the interface ($\pm$ 1°C) on the mass transfer coefficients is small except near the critical point of the solvent were a (20% AARD) change in mass transfer coefficients might result.

4.2.5 Mixing Effects

The calculation of natural convection forces depends strongly on the change in density, $\Delta\rho$, across the interface and the method used for estimating this property is important. The average density difference between the solid surface and the bulk ($\Delta\rho_m$) is the most important characteristic parameter in investigating

natural convection effects at supercritical conditions and this density difference is primarily due to differences in composition. The effect of mole fraction and pressure on $\Delta\rho_m$ at 35°C is shown in Figure II.11. In Figure II.11, the density difference, $\Delta\rho$, represents the difference in densities for a saturated solution (interface) and a solution at 0, 20, 40, 60 or 80% of saturation (bulk). The maximum effects occur in the region where the partial molar volume, $\bar{V}_1^{\infty}$ is smallest. Similar trends exist at different temperatures (25-55°C).

The relative density change due to the mixing on density has sometimes been estimated using the mixing expansivity which is defined by Estevez and Muller (1988) as follows:

$$K = \frac{1}{\rho}\left(\frac{\partial\rho}{\partial y_1}\right)_{T,P} = \frac{\overset{\curvearrowleft}{\rho}}{\rho} \qquad \text{(II-16)}$$

where $\overset{\curvearrowleft}{\rho}$ represents the density change with respect to the solute component at constant temperature and pressure. By using $\rho = M_m/V$ and $z = PV/RT$, Equation (II-16) becomes

$$K = -\frac{1}{z}\left(\frac{\partial z}{\partial y_1}\right)_{T,P} + \frac{M_1 - M_2}{M_m} = -\frac{\overset{\curvearrowleft}{z}}{z} + \frac{M_1 - M_2}{M_m} \qquad \text{(II-17)}$$

where M_1, M_2 and M_m are molecular weight of the solute and the solvent, and average molecular weight of the solution, respectively. The complete expression for K can be obtained by substituting an expression for $\overset{\curvearrowleft}{z}$ into Equation (II-17). Occasionally the absolute density due to the mixing is estimated by multiplying $\tilde{\rho}$ [= $(\partial\rho/\partial\ y_1)_{T,P}$] at infinite dilution times mole fraction, but the results of such a calculation can produce density values that are considerably in error compared to

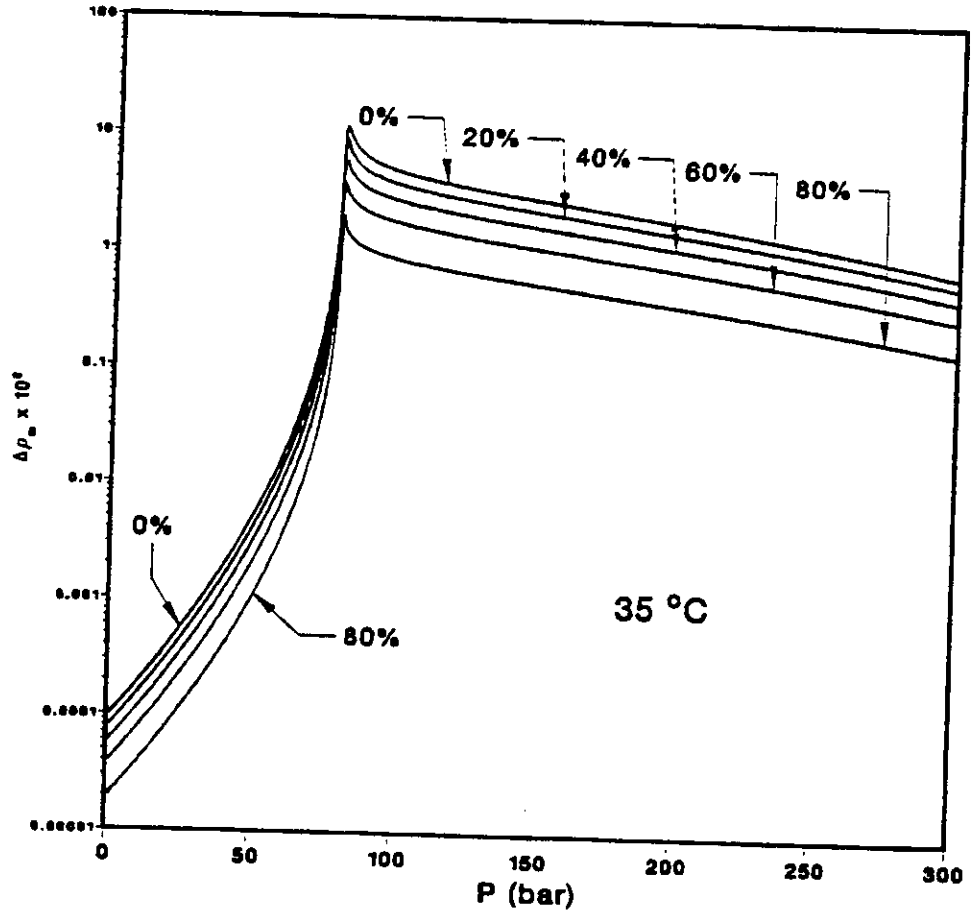

FIGURE II.11 Effects of Mole Fraction and Pressure on Density Difference ($\Delta\rho_m$) at 35 °C

the values estimated by an equation of state which is much more rigorous in nature. Figure II.12 shows the possible error in the estimation of the density change with composition when densities are obtained by $\hat{\rho}^{\infty} \times y_1$. In this figure ρ^* is the saturation density from an equation of state. For comparison, very low and high pressures (1 and 300 bar, respectively), and two pressures where the largest under-and overestimation of the equilibrium density occur are chosen. As expected, at all temperatures, the error in the calculation of equilibrium density is very small at low and high pressures (1 and 300 bar, respectively) but can be significant at pressures near the critical. At 35°C it shows that maximum error is about 10% (overestimation) at 81.18 bar and 6% (underestimation) at 78.97 bar. Even larger errors occur as the temperature approaches 31.04°C, the critical temperature. Clearly, an equation of state, such as the modified Peng-Robinson (1976) used in this study, gives superior estimations of the density.

4.2.6 Conclusions

Gas-solid mass transfer in the naphthalene-carbon dioxide system is explored for laminar flow under subcritical to supercritical conditions. This work represents the first experimental measurement and theoretical correlation of fluid-solid supercritical mass transfer coefficients in a packed bed. Both natural and forced convection are found to be important for supercritical mass transfer even though forced convection seems to be dominant at subcritical conditions. Correlations proposed for combined natural and forced convection in the laminar opposing flows regime can successfully predict the experimental results over the entire pressure and temperature range.

It has been found that at constant Re, the mass transfer coefficient is almost constant at low pressures below 60.8 bar. However, it increases dramatically near

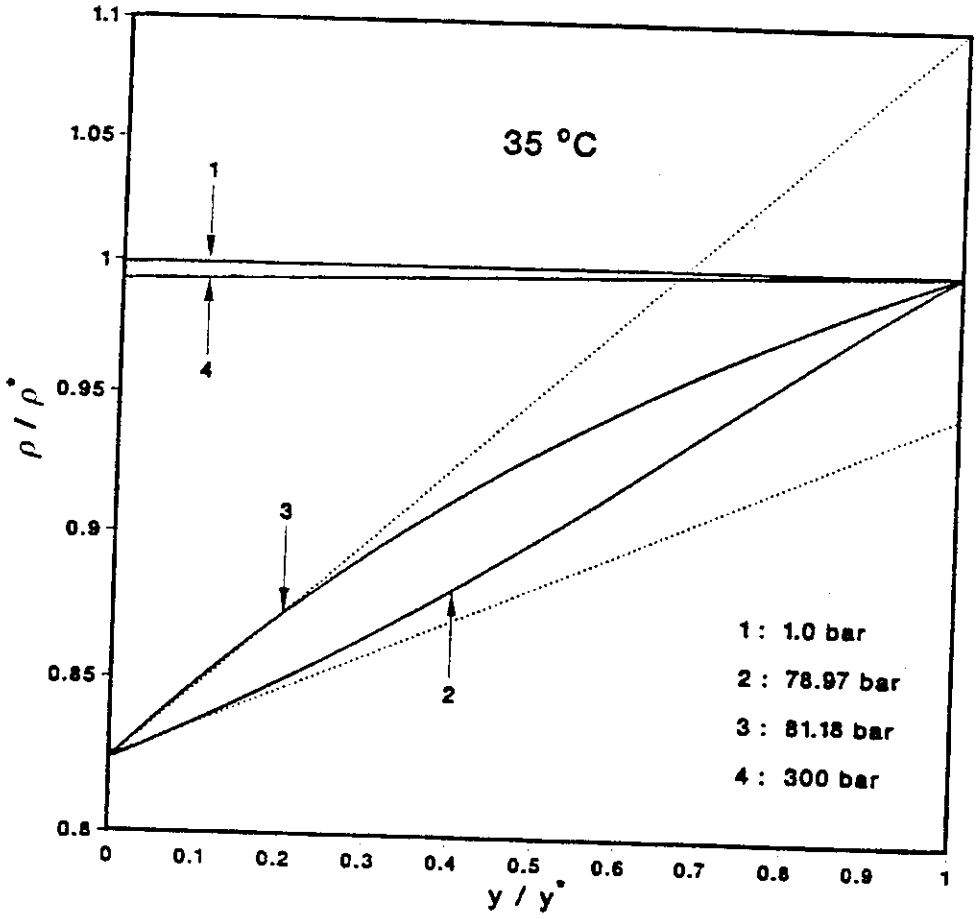

FIGURE II.12 The Possible Error in the Estimation of the Density of Naphthalene - Carbon Dioxide Equilibrium Mixture by Using $\bar{\rho}^{\infty}$ at 35 °C

the critical point, has a maximum value, then decreases gradually as the pressure increases beyond 100 bar. The mass transfer rate under supercritical conditions is much higher than at ambient conditions (25°C and 1.01 bar) for liquid-solid and gas-solid systems, due to strong natural convection effects. However, mass transfer enhancement by natural convection is not confined to the immediate vicinity of the solvent's critical point. This is due to the fact that the infinite dilution solute partial molar volumes ($\bar{V}_1^{\infty}$) have very large negative numbers over a range of temperatures and pressures. It is found that the range of temperatures and pressures where natural convection effects on mass transfer are strong can be located by the estimation of the density differences between the equilibrium mixture and pure supercritical fluid, as manifested in the Grashof number. Additionally, near critical conditions, the compressibility of the fluid begins to diverge and molecular level density fluctuations can occur and lead to additional convective contributions.

The density change with respect to the mole fraction of naphthalene at constant temperature and pressure, $[\hat{\rho} = (\partial\rho/\partial y)_{T,P}]$ is very high near the critical point of the solvent. Near the critical point the density change at the equilibrium mole fraction ($\bar{\rho}^{\infty}$*) is quite different from the density change at the infinite dilution limit ($\hat{\rho}^{\infty}$), and estimations of the density difference between the fluid at the solid surface and the fluid in the bulk supercritical phase, which are obtained by using $\hat{\rho}^{\infty}$ may result in inaccurate calculations. An equation of state should be used for estimating densities at all compositions.